DOI 10.1007/s12541-009-0040-1

Optimum Creep Feed Grinding Process Conditions for Rene 80 Supper Alloy Using Neural Network

Abbas Vafaeesefat[1,#]

1 School of Engineering, Department of Mechanical Engineering, Imam Hussein University, Tehran, Iran, 1698716111
Corresponding Author / E-mail: Abbas_v@yahoo.com,TEL: 9821-77104908, FAX: 9821-77104912

KEYWORDS: Neural network, Creep feed grinding, Process optimization, Workpiece burning, Nickel-based Supper alloys

Creep feed grinding is widely used in manufacturing supperalloy materials. These materials are usually used in aircrafts, gas turbines, rocket engines, petrochemical equipments and other high temperature applications. The objective of this paper is to model and predict the grinding forces of the creep feed grinding of these materials using the neural network. This model is then used to select the working conditions (such as depth of cut, the wheel speed and workpiece speeds) to prevent the surface burning and to maximize the material removal rate. The results show that the combined neural network and an optimization system are capable of generating optimal process parameters. The outcomes of the paper are now used to apply the optimal working conditions for grinding the turbine blades.

Manuscript received: November 17, 2008 / Accepted: February 2, 2009

NOMENCLATURE

v_s = wheel speed (m/s)
D = wheel diameter (mm)
a = grinding depth (mm)
v_w = workpiece speed (m/s)
b = width of cut (mm)
F_v = vertical force (N)
F_h = horizontal force (N)
Q_c = critical energy
k = thermal conductivity
ρ = material density
T_i = room temperature (16°C)
$T_{boiling}$ = boiling temperature (100° C)
r = surface covering rate
A_g = real contact area
l = length of contact area

1. Introduction

Grinding has traditionally been associated with small rates of material removal and fine finishing operations. Using an approach known as creep-feed grinding, a large-scale metal removal similar to milling can be achieved. Using this approach, higher material removal rates can be performed by selection of higher depth of cut and lower workpiece speed. The correct selection of the cutting conditions and the wheel specifications can provide a greater material removal rate and a finer surface quality.

In creep-feed grinding, the wheel depth of cut can reach as much as 6 mm. Higher cutting speed can cause the increase of force and cutting power, as well as a great heat generation in the grinding zone.[1] The heat can be reduced by using a high coolant flow rate and adequate pressure, which contributes to the reduction of the generated heat and easily remove the chips from the grinding zone.[2,3]

One of the most important applications of creep-feed grinding is the production of the aerospace parts used in jet engines such as turbine vanes, and blades where parts should have high strength to the fatigue loads and creep strains (see Fig. 1).[4] These parts are made from nickel-based super-alloys such as Inconel, Udimet, Rene, Waspaloy, and Hastelloy. They provide higher strength to weight ratio, and maintain high resistance to corrosion, mechanical thermal fatigue, and mechanical and thermal shocks.

Milling and broaching of these parts made of Nickel and Cobalt based super alloys are too difficult, and in some new materials with high toughness and hardness are impossible. An example of creep-feed grinding of the turbine blade with a shaped wheel is shown in Fig. 2.

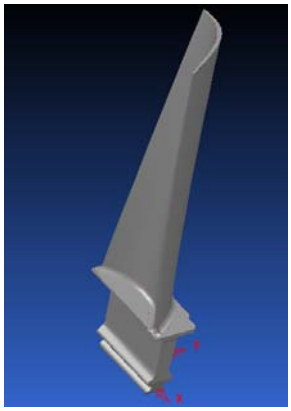

Fig. 1 Turbine blade

Fig. 2 Creep-feed grinding

The grinding process can cause the surface impairment such as surface burning mainly by the thermal damage.[5] Therefore, the main limitation of creep-feed grinding is found to be the surface burning. Therefore, the selection of working conditions to avoid the burning is very important.[6] These conditions can be defined by determining the grinding forces. The complex relationship between grinding forces and process parameters could not be easily expressed by analytical model. The analytical models are usually based on many assumptions and the coefficients are determined experimentally at specific configurations. Therefore, it is highly difficult to develop a comprehensive analytical model that considers all factors affecting the grinding forces.

Neural network architecture has become more and more important as an effective learning technique in pattern recognition, since it has strong abilities to learn, to self-organize information, and need only few specific requirements. These advantages have attracted much interest in research on machining processes.[7-9] Therefore, neural network model can be developed for a better understanding of the effects of process conditions on the grinding forces.

The objective of this paper is to determine process parameters, which satisfies the given limits, and maximizes the productivity at the same time. Neural network models can be combined with optimization methods in order to determine optimum grinding parameters. The experimental data obtained by a series of experiments performed on a Rene 80 supper alloy is first used to train a network. The implemented neural network algorithm of the force model is then used to predict the vertical and horizontal components of the grinding force. The predicted grinding forces will be further applied to the selection of the working conditions in avoidance of the workpiece burning and maximizing the material removal rate.

2. Artificial Neural Network

Neural networks are computational systems to simulate human brain in a simple and objective way. They have been used in diverse applications such as control, robotics, pattern recognition, forecasting, and manufacturing to model systems. Neural networks consist of a number of highly interconnected processing elements known as neurons. The neurons calculate the sum of computed weighted inputs and then apply a linear or non-linear function called transfer function to determine the outputs. The network is fed with a large amount of training data that represent the pattern attempting to be modelled. The weights are computed by an iterative method during the training process.

Neural Network modelling consists of two main steps: training and verification. During the training process, specified inputs together with the corresponding solved outputs are introduced to the neural system. A learning algorithm is implemented to adjust the weights between neurons in a way that the error between neural system outputs and targets comes to prescribed minimum. The goal of this learning algorithm is to get the outputs that are calculated using the weights of the neural network as close as possible to the desired output patterns for the training data. Thus, the system of neural networks learns these patterns and develops the ability to make predictions for newly introduced inputs.

The verification step is implemented to confirm the accuracy of the neural system in precisely predicting the solution to the new patterns. This is done by considering some verification data with known outputs to form the test set.

3. Experimental procedure

A series of experiments were performed on various wheel speeds, workpiece speed, and depth of cuts. The workpiece material is supperalloy Rene80. Workpiece dimensions are 30X20X12 mm made by investment casting process and the proper heat treatment was done for all samples. Creep-feed grinding was performed on 10 mm width of all experiments and grinding speed is set to 20, 25 and 30 m/s. Depth of cut was set to 1, 2 and 3 mm, and the workpiece speed was set to 0.5, 0.75, 1.0, and 1.25 mm/s. Vertical and horizontal components of grinding forces were measured by a dynamometer (Fig. 3).

In this work, a grinding wheel that is based on aluminium oxide with white synthetic bonding is used. The abrasive grit size number is 80. A continuous dressing with rate of 0.0004 mm/rev was

performed on the grinding wheel by a diamond roll. The wheel dressing is a parameter with a great impact on the grinding wheel topography and thus on the heat generation in the cutting process. Continuous dressing can minimize the wear and the frictional heat.

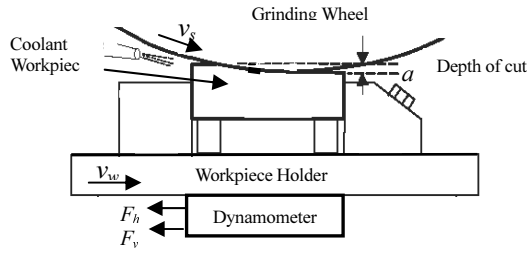

Fig. 3 Workpiece setting

In creep-feed grinding, the supply of coolant is usually the key requirement to keep the grinding zone temperature at a low level.[10] Therefore, the grinding area has to be cooled with the appropriate coolant. Nozzle pressure was set to 12 bar (100 litre/min) and the coolant was sprayed in contact area between the wheel and the workpiece.

Compared to up grinding, down grinding have lower normal (tangential) force ratio and less spindle load. This causes the generation of small wheel wear and lower grinding energy. Our primary results showed that up grinding causes the vibration of the workpiece and the fixture. This causes the creation of small hole on the workpiece surface. In the other hand, a better surface quality and a reduction of grinding forces by 12% were obtained in down grinding. Therefore, in this study, the experiments were performed in down grinding. Table 1 lists the working conditions of our experiments. Table 2 shows the composition of Rene 80 nickel based super alloy used in our experiments. The maximum vertical and horizontal forces measured with the dynameter are listed in table 3.

Table 1 Experiment settings

Devices	conditions
Grinding machine	Micro-cut 4-250 CNC- Machine capacity : 400 l * 300 w * 600 h-Machine power 48 KW
Grinding method	Down grinding
Grinding wheel	1- 54A80H15VPMF904W (400mm*32mm*127mm)
Grinding speed	v_s=20 m/s , 25 m/s , 30 m/s
Workpiece speed	v_w=1.25 mm/s, 1 mm/s, 0.75 mm/s, 0.5 mm/s
Depth of cut	a = 1 mm, 2 mm, 3 mm
width of cut	b = 10 mm
Dressing	Continuous dressing with rate of 0.0004 mm/rev
Workpiece	Material Rene80 12x30x20 with 42 Rockwell hardness
Coolant	Synthetic Fluids
Nozzle pressure of coolant	12 Bar, 100 litre/min

Table 2 The composition of RENE 80- Ni based super alloy

	C	Cr	Co	Mo	W	Ti	Al	Zr	B	S(Max)	Ni
Standard	0.15 0.19	13.7 14.3	9 10	3.7 4.3	3.7 4.3	4.8 5.2	2.8 3.2	0.02 0.1	0.01 0.02	0.007	Balance
Our material	0.17	14.1	9.5	4.0	4.0	5.1	3.0	0.06	0.015	0.01	

Table 3 The maximum vertical and horizontal forces measured with the dynamometer

NO	Working conditions				Experimental results	
	D (mm)	v_s (m/s)	a (mm)	v_w (mm/s)	Fv (N)	Fh (N)
1	395	30	2	1.25	306.8	105.6
2	394.67	30	2	1	268.4	92.4
3	394.27	30	2	0.75	235.3	83.1
4	393.76	30	2	0.5	212.8	75.6
5	393.03	30	1	1.25	206.4	73.4
6	392.70	30	1	1	176.9	62.3
7	391.79	30	1	0.75	150.2	55.
8	392.30	30	1	0.5	128.3	146.7
9	391.06	25	3	1	348.1	122.7
10	390.66	25	2	1	276.2	97.4
11	390.26	25	1	1	193.2	67.1
12	389.86	25	3	0.5	291.6	100.3
13	389.13	25	2	0.5	225.1	80.2
14	388.40	25	1	0.5	141.7	51.4
15	387.67	20	3	0.5	307.4	107.2
16	386.94	20	2	0.5	241.7	83.4
17	386.21	20	1	0.5	151.3	53.7
18	385.48	20	1	0.75	176.3	62.6
19	384.97	20	1	1	208.6	73.4

4. Structure of neural network model

In our approach, a three-layer neural network, one made up of an input layer, a hidden layer, and an output layer, was used to accurately model the grinding forces, providing a sufficient number of hidden neurons. The neuron number of the input layer of neural network is determined by the number of process parameters. The force model is developed using the presented experimental results that act as learning example. The four input variables used in the input layer are taken to be (1) the wheel speed, v_s (m/s), (2) the wheel diameter, D (mm), (3) the grinding depth, a (mm), (4) the workpiece speed, v_w (m/s). The wheel diameter is set as one of the input variables in the neural network model, since the variations in wheel diameter change the length of contact area, and, therefore, the grinding forces.

The neuron number of output layer is determined by the number of the objective indexes. Therefore, the vertical force, Fv (N), and the horizontal force, Fh (N) are two variables in the output layers. Fig. 4 shows the connection paths to and from one hidden layer neuron.

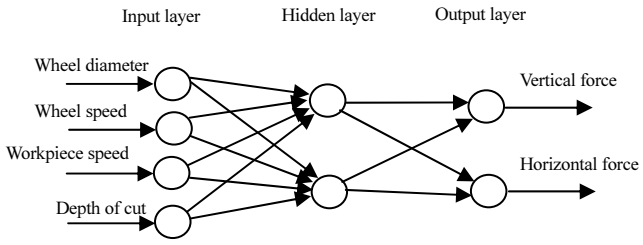

Fig. 4 Neural network structure used in modelling Grinding forces

Among other transfer functions, the tan-sigmoid transfer function was selected as the activation function for the hidden

layers, and linear transfer function was selected for the output layers. These selections are based on the minimum error found by these functions compared to other functions. Using these two activation functions, a given output, Y, based on the inputs, X, and the connection weights, W_1 and W_2, is given by

$$Y = B_2 + W_2 * f(W_1 * X + B_1) \quad (1)$$

where B_1 and B_2 are bias of the neuron, which is simply an extra degree of freedom to adjust allowing the input-output relationship to be learned accurately during training.

During training, a number of input-output pairs are given to the network and the weights of the connection paths are adjusted. The most common method to adjust the weights of the connection paths is through the back-propagation algorithm that is used in our work. In this approach, the effects of the errors are swept backwards through the neural network to obtain a square error derivative for each computational neuron. The gradient is then calculated for all of the square error derivatives allowing the weights to be updated using Levenberg-Marquardt method in each iteration. The process is repeated for all of the training examples in specified number of iterations.

5. Modeling grinding forces using neural network

The neural network model shown in Fig. 4 is used to predict the grinding forces. The node number of the hidden layer was determined by train trials and the final value obtained was three that made the configuration of neural network as 4–2–2. The learning rate is 0.01. Among the samples obtained by experimental results, 16 samples were used to train the neural network. The remaining three samples were then used to test the performance of the neural network.

Table 4 Comparison between the experimental and neural network results

NO	Working conditions				Neural Network results		
	D (mm)	v_s (m/s)	a (mm)	v_w (mm/s)	Fv (N)	Fh (N)	%*Error*
1	395	30	2	1.25	296.4755	103.2689	2.4665
2	394.67	30	2	1	267.5366	93.6148	1.0220
3	394.27	30	2	0.75	237.9509	83.6190	0.7043
4	393.76	30	2	0.5	210.5238	74.3259	1.6073
5	393.03	30	1	1.25	04.4195	72.0607	1.7467
6	392.70	30	1	1	177.4305	63.0056	1.0174
8	391.79	30	1	0.5	131.2160	47.4758	1.7064
9	391.06	25	3	1	54.1182	122.9479	.5044
10	390.66	25	2	1	283.6178	98.9799	1.7700
12	389.86	25	3	0.5	290.0974	101.2746	0.6645
13	389.13	25	2	0.5	226.6018	79.7719	0.3336
14	388.40	25	1	0.5	44.8586	52.0948	1.4383
15	387.67	20	3	0.5	304.5912	106.1859	0.9484
17	386.21	20	1	0.5	159.1120	56.9092	5.5486
18	385.48	20	1	0.75	181.5197	64.3662	2.7604
19	384.97	20	1	1	208.9572	73.5922	0.2499

The predicted and experiment results and process parameters are shown in Table 4. The result indicates that the neural network has a good performance, and it can accurately map the relationship between the grinding forces and process parameters. The implemented neural network algorithm is used to predict three testing examples. The testing results as compared to the experimental results are listed in table 5. It shows that the grinding forces can be forecasted effectively using the neural network.

Table 5 Evaluation of neural network for the new data

NO	Working conditions				Neural Network results		
	D	v_s	a	v_w	Fv	Fh	%*Error*
7	392.30	30	1	0.75	154.44	55.335	0.3509
11	390.26	25	1	1	191.9255	67.8428	0.8743
16	386.94	20	2	0.5	242.89	85.290	1.0145

6. Optimal working conditions

The optimal working conditions are obtained by maximizing the material removal rate (MRR). Increasing the depth of cut and workpiece speed causes the increase of MRR. However, this increases the workpiece temperature and cause the surface burning. Therefore, the constraint in our optimization model is the surface burning.

The heat generated in the grinding zone is conducted to the workpiece, the grinding wheel, the coolant, and the grinding chips.[11,12] The partition of the grinding heat to the different heat sectors varies with process conditions. In order to work within a safe regime without causing any thermal damage to the workpiece, the controlling factors when designing a grinding process have to be carefully defined.[13]

The workpiece burning occurs with the abrupt increase of grinding force and a sudden rise of the workpiece temperature. The present coolant will cool the workpeice surface rapidly as the workpiece leaves the grinding zone. This is similar to the workpiece quenching phenomenon. These phenomena will cause the workpiece surface hardening and, therefore, cracks on workpiece surface. Thus, the workpiece temperature becomes one of the main factors affecting the surface quality.

The grinding energy when the fluid begins to cause boiling is defined as the critical grinding energy for the workpiece burning. The critical issue in the creep-feed grinding is to prevent the coolant to boil. When the coolant reaches the boiling point, the proper heat transferring is prevented. Therefore, when the coolant reaches to the boiling point, more heat will build up in the grinding zone that causes the workpiece burning. Based on the researches done by Wang and Kou,[14] the critical energy Q_c of grinding can be defined as a function of boiling temperature:

$$Q_c = \frac{1}{R_f}\sqrt{\frac{\pi(k\rho c)_f v_s}{4(aD)^{0.5}(1-r)^{0.5}}}(T_{boiling} - T_i) \quad (2)$$

$$R_f = \left[1 + \left[\frac{1}{(1-r)^{0.5}} \cdot \frac{(k\rho c)_w v_w}{(k\rho c)_f v_s}\right]^{0.5} + \left[\frac{r^{0.5}}{(1-r)^{0.5}} \cdot \frac{(k\rho c)_g}{(k\rho c)_f}\right]^{0.5}\right]^{-1}$$

where k, ρ, c, v_w, D, a, v_s, T_i, $T_{boiling}$, are thermal conductivity, material density, specific heat, workepiece speed, wheel diameter, depth of cut, wheel speed, room temperature (16°C), and boiling temperature (about 100° C), respectively.

Indices *w, f,* and *g* represent the workpiece, fluid, and the grain, respectively. R_f is the partition of total energy Q_t transferred to the fluid. In addition, r is surface covering rate $r=A_g/A_{total}$ where $A_{total}=l*b$ is total grinding surface, A_g is the real contact area, and l is the length of contact area ($l=\sqrt{a\cdot D}$). Malkin[15] measured this ratio and found that this ratio is very small from 0.01 to 0.02. In our approach, the surface covering rate, *r,* is set to 0.01.

To define safe working conditions, the total energy has to be defined. When the total energy is greater than the critical energy, the surface burning may occur. Assuming the uniform energy over the whole contact area, the total energy is defined by

$$Q_t = \frac{Ft \cdot V_s}{lb} \tag{3}$$

where Ft is the tangential force, and b is the width of cut. The tangential force in down grinding is obtained from the horizontal grinding force Fh, and the vertical grinding force Fv by (Fig. 5):

$$Ft = Fv \sin\theta_m + Fh\cos\theta_m \tag{4}$$

where θ_m is mean rotation of contact length $\theta_m=\sqrt{a/D}$.

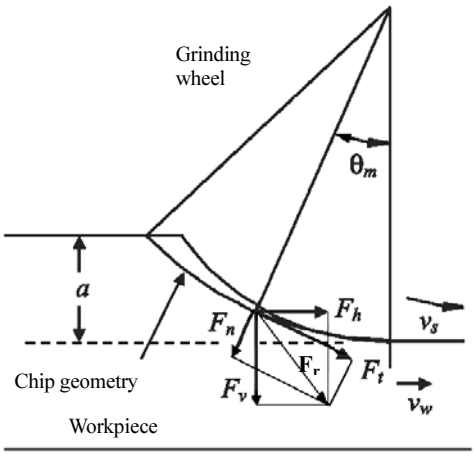

Fig. 5 Grinding forces

Having the working conditions and material properties (Table 6), the critical and total energies are calculated using equations 2 and 3, respectively. Experimental results show that the workpiece surface is burned in case number 1 and 9 where the total energy is greater than the critical energy (Table 7). This shows a good agreement between the adaptive thermal theory and experiments results. Therefore, the adaptive thermal theory can be used to predict the occurrence of surface burning.

Table 6 Material properties of the coolant, Rene80, and the wheel

	Coolant	Rene80	Wheel
$k(w/m^{\circ}C)$	0.625	25.23	135
$\rho(kg/m^3)$	991	8170	1750
$c(J/kg^{\circ}C)$	4071	962.964	720

Table 7 The critical and total energies of experiments

NO	Working conditions				Experimental results	
	D (mm)	v_s (m/s)	a (mm)	v_w (mm/s)	Q_C (W/mm^2)	Q_t (W/mm^2)
1	395	30	2	1.25	12.47	13.57
2	394.67	30	2	1	12.44	11.88
3	394.27	30	2	0.75	12.43	10.64
4	393.76	30	2	0.5	12.41	9.68
5	393.03	30	1	1.25	14.83	12.67
6	392.70	30	1	1	14.81	10.77
7	392.30	30	1	0.75	14.80	9.48
8	391.79	30	1	0.5	14.77	8.05
9	391.06	25	3	1	10.31	11.14
10	390.66	25	2	1	11.43	10.46
11	390.26	25	1	1	13.59	9.72
12	389.86	25	3	0.5	10.28	9.17
13	389.13	25	2	0.5	11.39	8.61
14	388.40	25	1	0.5	13.57	7.42
15	387.67	20	3	0.5	9.25	7.85
16	386.94	20	2	0.5	10.21	7.23
17	386.21	20	1	0.5	12.15	6.24
18	385.48	20	1	0.75	12.19	7.28
19	384.97	20	1	1	12.22	8.56

7. Results and discussion

The neural network developed in the previous section can now be used to predict the grinding forces and the total energy. In addition, the critical grinding energy of the workpiece burning is obtained by equation 2.

The working conditions where the predicted total grinding energy and critical grinding energy lie together can be regarded as the critical working conditions under the limitation without occurrence of the workpiece burning. Therefore, the predicted grinding energy with the adaptive thermal models can be used to forecast the workpiece burning.

The grinding energies variations versus working conditions are shown in Fig. 6 and 7. They show that the critical energy is almost unchanged with the different workpiece speed, but the total energy is increased by the workpiece speed. The critical energy becomes greater at smaller depth of cut and larger wheel speed. The larger critical grinding energy means that a greater heat generated in the grinding zone is permitted without workpiece burning. Moreover, the predicted total grinding energy becomes greater as grinding depth, wheel speed, and workpiece speed are increased. The greater the total grinding energy reveals the larger grinding heat and grinding forces generated during grinding process. The reduction of the depth of cut or the workpiece speed can lower the grinding energy.

Based on the consideration of more working efficiency, the working conditions can be adjusted to obtain a higher material removal rate (MRR). The neural network was used to determine a set of optimal inputs. In the present case of optimization of creep feed grinding process, the cost function which is to be maximized,

is the MRR and the constraint is the surface burning. The optimization problem to maximize MRR while avoiding the surface burning can be defined by

$$\begin{aligned} \max \quad & MRR = a * v_w \\ S.t. \quad & Q_t \le Q_c \\ & 1 \le a \le 3 \\ & 0.5 \le v_w \le 1.25 \\ & 20 \le v_s \le 30 \end{aligned} \tag{5}$$

Critical energy and total energy Q_t are calculated by equations 2 and 3 respectively. The above optimization problem was solved by nonlinear constrained optimization and the optimal working conditions to maximize MRR are found to be a=2.665 mm, v_s=20.5 m/s, v_w=1.05 mm/s for D=390 mm. The MRR with these parameters is 2.8 mm^2/s. These parameters are now used experimentally for creep feed grinding of Rene 80 supper alloy.

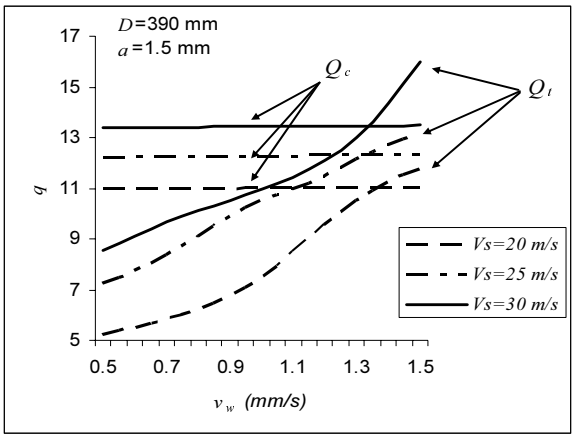

Fig. 6 Grinding energies Q_t and Q_c versus workpeice speed v_w in different wheel speed v_s

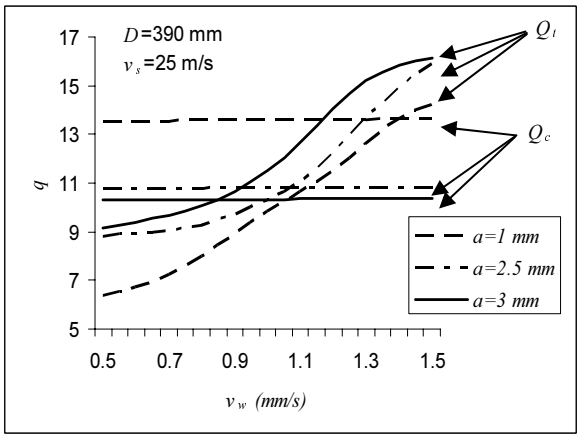

Fig. 7 Grinding energies Q_t and Q_c versus workpeice speed v_w in different depth of cut a

8. Conclusion

In this paper, the parameters involved in the creep feed grinding of nickel-based superalloy materials are investigated. In order to predict the grinding forces using neural network, a series of experiments is performed on supperalloy Rene80 to define the appropriate working conditions. The neural network technique has been shown as an effective method to model the complex relationship between the process conditions and the grinding forces. The results indicate that the presented neural network of one hidden layer with three neurons was successful in predicting the grinding forces. The predicted grinding forces with the adaptive thermal models are used to optimize the MRR while avoiding the workpiece burning. The neural network model and optimization methods proposed in this paper show the great potential in complicated industrial applications.

References

1. Bianchi, E. C. and Silva, E. J., "The grinding wheel performance in the transverse cylindrical grinding of an Eutetic Alloy," Material Research, Vol. 5, No. 4, pp. 433-438, 2002.
2. Wang, S.-B. and Kou, H.-S., "Cooling Effectiveness of cutting fluid in creep feed grinding," International Communications in Heat and Mass Transfer, Vol. 24, No. 6, pp. 771-783, 1997.
3. Webster, J., Brinksmeier, E., Heinzel, C., Wittmann, M. and Thoens, K., "Assessment of grinding fluid effectiveness in continuous-dress creep feed grinding," CIRP Annals - Manufacturing Technology, Vol. 51, No. 1, pp. 235-240, 2002.
4. Sunarto, Y. I., "Creep feed profile grinding of Ni-based superalloys with ultrafine-polycrystalline cBN abrasive grits," Precision Engineering, Vol. 25, No. 4, pp. 274-283, 2001.
5. Alagumurthi, N., Palaniradja, K. and Soundararajan, V., "Cylindrical grinding - A review on surface integrity," International Journal of Precision Engineering and Manufacturing, Vol. 8, No. 3, pp. 24-44, 2007.
6. Xu, X. P., Yua, Y. Q. and Xub, H. J., "Effect of grinding temperatures on the surface integrity of a nickel-based superalloy," Journal of Materials Processing Technology, Vol. 129, No. 1-3, pp. 359-363, 2002.
7. Jain, R. K. and Jain, V. K., "Optimum selection of machining conditions in abrasive flow machining using neural network," Journal of Materials Processing Technology, Vol. 108, No. 1, pp. 62-67, 2000.
8. Wang, Z., Willett, P., DeAguiar, P. R. and Webster, J., "Neural network detection of grinding burn from acoustic Emission," International Journal of Machine Tools & Manufacture, Vol. 41, No. 2, pp. 283-309, 2001.
9. Jianjun, Y., Yifeng, G., Baiyang, J., Bin, Y. and Jinxiang, D., "Applying an artificial neural network to the control system for electrochemical gear-tooth profile modifications," International Journal of Precision Engineering and Manufacturing, Vol. 8, No. 4, pp. 27-32, 2007.
10. Andrews, C., Howes, T. and Pearce, T., "Creep feed grinding," Rinehart & Winston, 1985.

11. Jin, T. and Stephenson, D. J., "Investigation of the heat partitioning in high efficiency deep grinding," International Journal of Machine Tools & Manufacture, Vol. 43, No. 11, pp. 1129-1134, 2003.

12. Maksoud, T. M. A., "Heat transfer model for creep-feed grinding," Journal of Materials Processing Technology, Vol. 168, No. 3, pp. 448-463, 2005.

13. Gin, T. and Stephenson, D. J., "Investigation of the heat partitioning in high efficiency deep grinding," International Journal of Machine Tools and Manufacture, Vol. 43, No. 11, pp. 1129-1134, 2003.

14. Wang, S.-B. and Kou, H.-S., "Selections of working conditions for creep feed grinding. Part(II): Workpiece temperature and critical grinding energy for burning," International Journal of Advanced Manufacturing Technology, Vol. 28, No. 1-2, pp. 38-44, 2006.

15. Malkin, S. and Cook, N. H., "The wear of grinding wheels, Part 1 - Attritious Wear," Journal of Engineering for Industry, Trans. ASME, Vol. 93, No. 4, pp. 1120-1128, 1971.